

Cite this: *Environ. Sci.: Nano*, 2014, 1, 302

## Environmental science and engineering applications of nanocellulose-based nanocomposites

Haoran Wei,<sup>abc</sup> Katia Rodriguez,<sup>bd</sup> Scott Rennekar<sup>bd</sup> and Peter J. Vikesland<sup>\*abc</sup>

Compared with cellulose, the primary component of the paper we use every day, nanocellulose has a much smaller diameter (typically  $<10$  nm) that renders it many unique properties. Amongst many others, these properties include high mechanical strength, large surface area and low visual light scattering. Nanocellulose can be obtained by disintegration of plant cellulose pulp or by the action of specific types of bacteria. Once produced, nanocellulose can be used to make transparent films, fibers, hydrogels, or aerogels that exhibit extraordinary mechanical, thermal, and optical properties. Each of these substrates is a suitable template or carrier for inorganic nanoparticles (NPs), thus enabling production of nanocomposites that possess properties of the two constituents. In this review, we focus on the preparation of nanocellulose, nanocellulose films, and nanocellulose papers, and introduce nanocellulose-based nanocomposites and their environmental applications.

Received 5th April 2014,  
Accepted 25th June 2014

DOI: 10.1039/c4en00059e  
[rsc.li/es-nano](http://rsc.li/es-nano)

### Nano impact

In this tutorial review, we summarize recent progress in the preparation and the application of nanocellulose-based nanocomposites. This is the first review paper that discusses the application of these novel nanomaterials to address environmental challenges. It is our intent that this review will provide inspiration for environmental scientists, environmental engineers, and others who are eager to develop new tools to solve emerging environmental challenges.

## Introduction

Nanocellulose is considered a sustainable nanomaterial due to its ready availability, biodegradability, and biocompatibility. When it is interwoven, nanocellulose can form highly porous and mechanically strong bulk materials such as nanocellulose papers, films, or aerogels.<sup>1–3</sup> These porous materials can be used as substrates for impregnation of a range of different nanomaterials. The resultant nanocomposites combine the advantages of both nanomaterials and perform synergistically. As of this writing, metal (Au, Ag, Pd, Ni, etc.), mineral ( $\text{Ca}_x(\text{PO}_4)_y$ ,  $\text{CaCO}_3$  and montmorillonite), and carbon (carbon nanotube and graphene) nanomaterials have been incorporated into nanocellulose substrates,<sup>4–8</sup> and the extraordinary electrical, optical and catalytic properties of these nanocomposites have been extensively demonstrated. Furthermore,

a growing body of evidence indicates nanocellulose can act as a hard template for the synthesis of novel nanomaterials.<sup>9,10</sup> In previous review papers, the nanocellulose-based nanocomposites primarily discussed are nanocellulose-reinforced polymers, for which nanocellulose was added into the polymer matrix.<sup>11–14</sup> However, this present review paper is focused on the preparation and applications of nanocellulose/inorganic NP nanocomposites that utilize nanocellulose as a novel carrier to house different types of inorganic NPs. Recent reviews have discussed the progress made in the development of nanofibril/inorganic NP nanocomposites. But these reviews either focused only on a specific kind of nanocellulose or talked about a wide range of biogenic nanofibrils.<sup>15–17</sup> In addition, these reviews did not examine the specific applications of nanocellulose-based nanocomposites within environmental science and engineering. From the point-of-view of an environmental scientist, nanocellulose-based nanocomposites have shown potential for applications in drinking water filtration,<sup>18–20</sup> catalytic degradation of organic pollutants,<sup>21–23</sup> absorbents to remove spilt oil from water,<sup>24</sup> monitoring waterborne pathogens and organic contaminants,<sup>25–27</sup> and superior energy conversion devices.<sup>28,29</sup> In this review, the possible applications of

<sup>a</sup> Department of Civil and Environmental Engineering, Virginia Tech, Blacksburg, Virginia, USA. E-mail: [pvikes@vt.edu](mailto:pvikes@vt.edu); Tel: +1 (540) 231 3568

<sup>b</sup> Virginia Tech Institute of Critical Technology and Applied Science (ICTAS) Sustainable Nanotechnology Center (VTSuN), Blacksburg, Virginia, USA

<sup>c</sup> Center for the Environmental Implications of Nanotechnology (CEINT), Duke University, Durham, North Carolina, USA

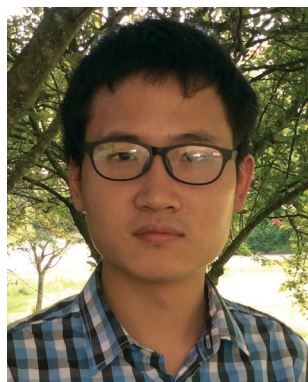
<sup>d</sup> Department of Sustainable Biomaterials, Virginia Tech, Blacksburg, Virginia, USA



nanocellulose-based nanocomposites are limited to a narrow area – environmental science and engineering, which is a distinct angle from the extent reviews. It may provide guidance for environmental scientists and engineers who are looking for new materials to address the emerging environmental challenges.

Nanocellulose exists in a number of forms that have been given a variety of names. These names include: homogenized cellulose pulps that are commonly described as microfibrillated cellulose (MFC) or nanofibrillated cellulose (NFC); acid hydrolyzed cellulose whiskers, known as nanocrystalline cellulose (NCC) or cellulose nanocrystal (CNC); and bacterially produced cellulose or bacterial cellulose (BC).<sup>35</sup> The relationship between these different kinds of nanocellulose is illustrated in Scheme 1. MFC consists of bundles of microfibrils, which are the primary constituents of the parent cellulose. In contrast, NCC has much lower aspect ratios than

MFC due to the partial hydrolysis of amorphous portions of the microfibril. Nanocelluloses can be derived from plants (e.g., wood, wheat straw, potato pulp, etc.<sup>30,36–39</sup>) or via bacterial processes.<sup>40</sup> Generally, plant-derived nanocellulose is produced by the top-down mechanical and/or chemical treatment of cellulosic precursors. In contrast, bacterial nanocellulose is produced by the direct action of specific bacterial strains belonging to genus such as *Achromobacter*, *Alcaligenes* and *Gluconacetobacter* (previously known as *Acetobacter*) among which only *Gluconacetobacter xylinus* has been shown to produce BC at commercial production levels.<sup>41,42</sup> Electrospinning and regeneration of cellulose acetate are alternative methods to obtain nanocellulose.<sup>43</sup> The final radial diameter of nanoscale cellulose is dependent on source and isolation processes, but typically the diameter of wood derived cellulose ranges from 10–40 nm when mechanically fibrillated, to 4–10 nm for NCCs, and 2–5 nm for chemical/mechanical iso-



Haoran Wei

*Haoran Wei received a MS (July 2013) in Environmental Engineering from Tsinghua University after receiving his BS (June 2010) in Environmental Engineering from Shandong University. He is currently a Ph.D. candidate in Civil and Environmental Engineering at Virginia Tech. His research interests are in the development of nanotechnology-based biosensors for detection of waterborne pathogens or contaminants.*



Katia Rodriguez

*Katia Rodriguez earned her B.S. in chemical engineering and M.S. in wood science and forest products from the University of Guadalajara, Mexico in 2002 and 2005, respectively. She graduated from the Ph.D. program in materials science and engineering at Virginia Tech in 2011. Currently, she is a postdoctoral research fellow at Virginia Tech. Her research experience includes fabrication of medical devices from nanocellulose.*



Scott Renneckar

*program is centered on creating advanced renewable materials derived from plants and trees.*

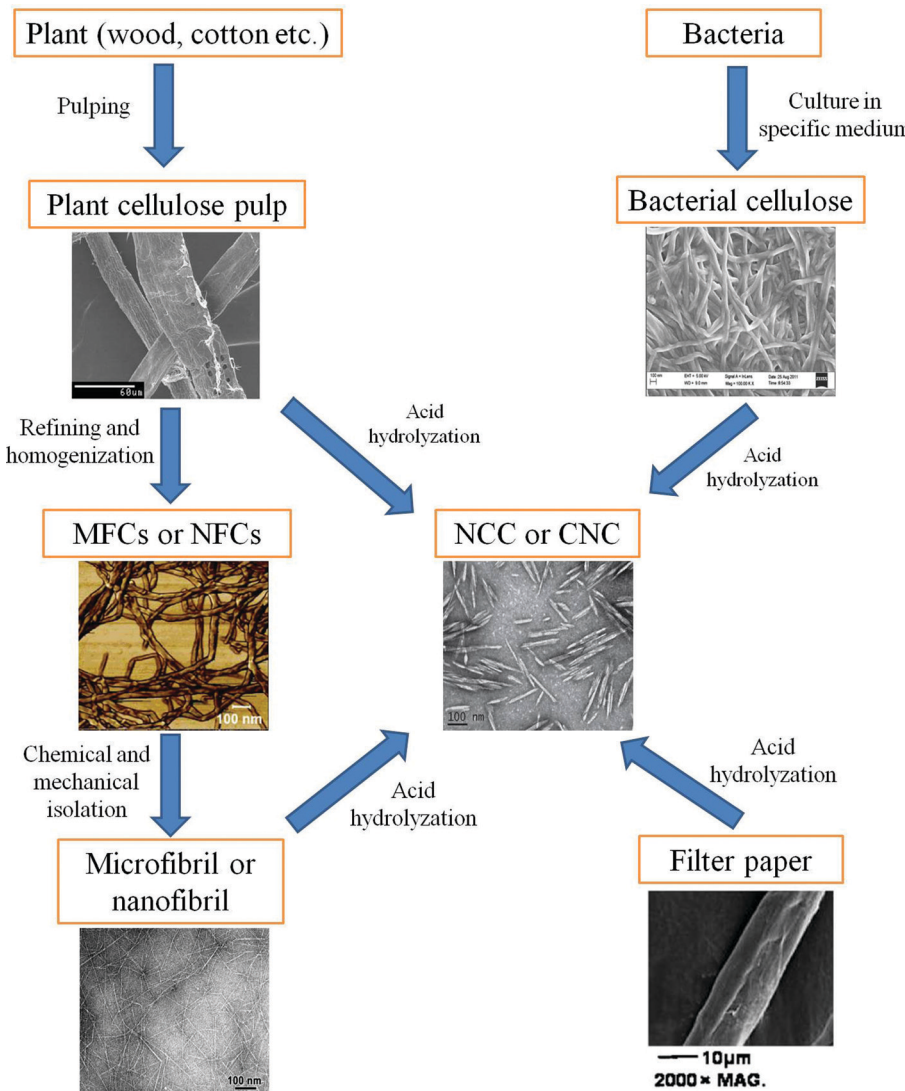
*Scott Renneckar is an Associate Professor of Wood Science at The University of British Columbia. Prior to joining UBC he worked with nanocellulose materials for the past decade at Virginia Tech as a faculty member in the Department of Sustainable Biomaterials. He studied Wood Science for his BS (1997) and PhD (2004) degrees from Virginia Tech, and his MS (1999) degree from the University of California, Berkeley. His research*



Peter J. Vikesland

*Peter J. Vikesland is a Professor of Civil and Environmental Engineering at Virginia Tech. He received his BA (1993) in Chemistry from Grinnell College and obtained his MS (1995) and Ph.D. (1998) in Civil and Environmental Engineering from the University of Iowa. After completing a postdoctoral fellowship at Johns Hopkins University he joined the faculty at Virginia Tech in 2002. Vikesland is a NSF CAREER awardee and currently serves as the Director of the Virginia Tech Sustainable Nanotechnology Interdisciplinary Graduate Education Program. His research group is interested in the development of nanotechnology-based approaches for the protection of water and air.*





**Scheme 1** Relationship between different kinds of nanocelluloses. Images from ref. 30–34.

lation. Nanocellulose exhibits high stiffness (≈one order of magnitude less than that of single-walled carbon nanotubes), low thermal expansion and low density, properties that are similar to those of carbon nanotubes.<sup>44</sup>

Nanocellulose can be used to reinforce polymers, paper, and membranes.<sup>30,45,46</sup> Properly prepared nanocellulose can also be used in a variety of medical applications. Bacterial nanocellulose, in particular, is a promising material for use in implants and as a tissue engineering scaffold because it does not require extensive processing to remove hemicellulose and lignin contaminants.<sup>47</sup> Nanocellulose can be readily modified into a range of different forms, such as papers, transparent films, aerogels, hydrogels, and even spherical particles.<sup>48</sup> The most common way to make nanocellulose paper or film is to filter a nanocellulose suspension on a filter or cast the suspension on a plate and then dry it. The drying method employed plays a crucial role in the quality of the papers and films obtained. Drying under vacuum with constraint clamping is often adopted to prevent wrinkling.<sup>2</sup>

In the following sections, we introduce the preparation of nanocellulose, nanocellulose papers, and nanocellulose films. The review then concludes with a discussion of the production of nanocellulose-based nanocomposites and their potential environmental applications.

## Preparation of nanocellulose

MFCs are often produced by high-shear mechanical treatment of micron-sized cellulose pulp that has been pre-treated with bleaching agents to remove lignin and hemicellulose.<sup>49</sup> Typical mechanical treatments incorporate refining and high-pressure homogenization. In the refining step, which is the same as that used by the paper industry, the fibers are sheared, cut, and frayed between two serrated disks. In the homogenization step the fibers are subjected to a large pressure drop with shearing and impact forces. This combination of forces promotes fibrillation of the cellulose fibers and results in the final MFC products.<sup>30</sup> In addition to

mechanical homogenization, ultrasonic techniques have also been found to be useful for MFC preparation.<sup>50</sup> It is generally believed that the more the MFCs are disintegrated, the better their resulting reinforcement performance. Accordingly, intensive efforts have been made to increase the degree of MFC fibrillation. Some researchers enhanced MFC disintegration by repeated homogenization.<sup>51</sup> However, when the number of homogenizations exceeds a certain value, the degree of fibrillation no longer continues to increase even though the input energy is increased substantially. A recent life cycle assessment indicated that the energy requirement for homogenization was approximately 110 MJ lower compared to sonication.<sup>52,53</sup> For this reason, alternative methods for homogenization have been tested, such as pretreatment of the pulp prior to homogenization to further disintegrate the nanocellulose and reduce the required energy input.<sup>39,52,54</sup> Pääkkö *et al.* pretreated cellulose pulp with endoglucanases before homogenization. The resultant nanocelluloses contained both 10–20 nm MFCs and 5 nm microfibrils. Because of the mild enzymatic hydrolysis prior to mechanical treatment, the required energy input was greatly reduced.<sup>55</sup> Furthermore, by adjusting the enzyme dose and the homogenization time, MFCs with different molar mass can be obtained.<sup>56</sup>

It is typically desirable to isolate individual microfibrils to maximize NP surface area to volume. Although a variety of methods have been used to fibrillate MFCs, the isolation of single microfibrils in suspension remains a challenge.<sup>45</sup> One way to isolate microfibrils is to utilize 2,2,6,6-tetramethyl-piperidine-1-oxyl radical (TEMPO) mediated oxidation to introduce carboxylic groups to the cellulose surface. Saito *et al.* used TEMPO oxidation to treat cotton linter with NaBr as a catalyst and NaOCl as an oxidant. The resultant microfibrils had 0.7 mmol g<sup>-1</sup> carboxylic groups and 0.3 mmol g<sup>-1</sup> aldehyde groups on the cellulose surface.<sup>57</sup> A shortcoming of this study was the low degree of oxidation because there were still 0.3 mmol g<sup>-1</sup> aldehyde groups that were not oxidized into carboxylic groups. When the number of carboxylic groups exceeds 1 mmol g<sup>-1</sup>, the microfibrils separate easily.<sup>32</sup> The same group overcame this shortcoming by using TEMPO/NaOCl/NaClO<sub>2</sub> system under neutral conditions. Because the aldehyde groups were oxidized by NaClO<sub>2</sub> to carboxylic groups, colloids of individual microfibrils were produced (Fig. 1).<sup>44</sup> Individual microfibrils can also be obtained by applying the TEMPO/NaBr/NaOCl treatment to never-dried native celluloses. Never-dried celluloses are better than once dried samples because the latter are known to irreversibly lose surface accessibility and reactivity as a result of drying.<sup>32</sup> However, after obtaining the proper degree of oxidation, once-dried cellulose will fibrillate similar to never-dried pulp.<sup>58</sup>

NCCs are highly crystalline nanocelluloses with lower aspect ratios than MFCs that can be prepared by mineral acid hydrolysis of plant cellulose pulp, filter paper, and BC.<sup>59–61</sup> At low concentrations, the NCCs randomly orient in water and form an isotropic phase. When the concentration exceeds a

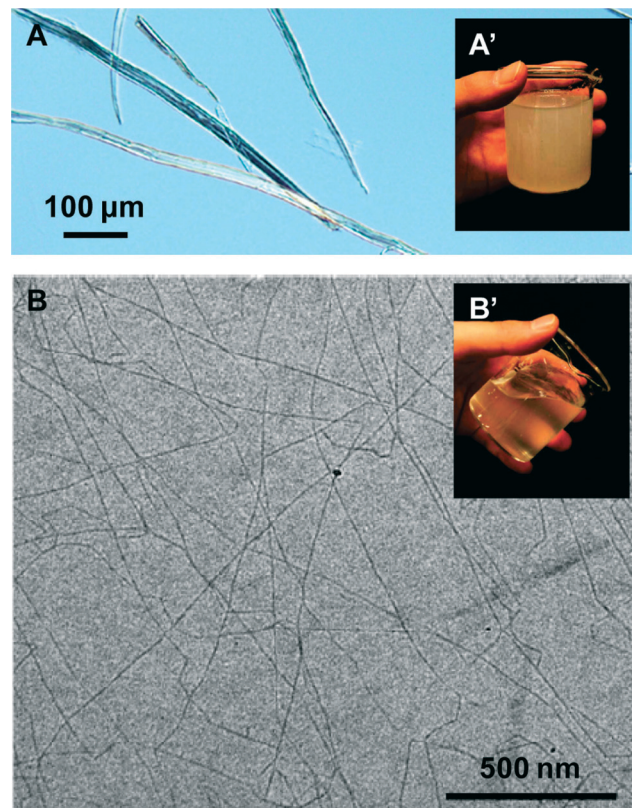


**Fig. 1** a) Optical micrograph of TEMPO-oxidized cellulose fiber; b) TEM of the TEMPO-oxidized cellulose fiber.<sup>44</sup> Reprinted with permission from T. Saito, M. Hirota, N. Tamura, S. Kimura, H. Fukuzumi, L. Heux, A. Isogai, Individualization of nano-sized plant cellulose fibrils by direct surface carboxylation using TEMPO catalyst under neutral conditions, *Biomacromolecules*, 2009, **10**(7), 1992–1996. Copyright 2014 American Chemical Society.

critical value, a nematic/chiral nematic phase forms and the resultant chiral nematic order can be maintained after evaporation of water.<sup>62</sup> This property has been exploited in combination with other additives to create structurally colored films.<sup>10,63</sup> The properties of the final microcrystals are determined by the preparation conditions. Only at moderate hydrolysis temperatures and times can the chiral nematic phase be achieved as these conditions influence the microcrystal size and substitution of sulfate ester groups on the surface.<sup>64</sup>

## Preparation of nanocellulose paper and film

The method for preparation of nanocellulose paper is built upon the common methods for paper production employed by the paper industry. Generally speaking, a nanocellulose suspension is filtered through a porous substrate and then the cellulose mat obtained on the substrate is pressed and dried to make paper. The only differences between nanocellulose paper and common cellulose paper are the diameter of the fibers used and the interstices (e.g., porosity) of the



resultant paper. Because the nanocellulose diameter and the interstices in the nanocellulose paper are much smaller than the wavelength of visible light, less scattering occurs when light illuminates nanocellulose paper. For this reason, transparent nanocellulose papers can be readily produced. Sehaqui *et al.* made nanocellulose papers by filtration of 0.2% MFC suspension through a 0.65  $\mu\text{m}$  pore size filter membrane. The wet gel cake was clamped between woven metal cloth and carrier board and then dried at 363 K and 70 mbar in a Rapid-Kothen semiautomatic sheet former. The papers obtained by this rapid method are flat and transparent and show greater mechanical strength than those prepared by time-consuming suspension casting methods.<sup>2</sup> Hu *et al.* adopted a similar approach to make a transparent nanocellulose paper and investigated the optical properties of the paper.<sup>65</sup> The light transmittance of the paper was about 90% when the light detector was 0 mm away from the paper. However, when this distance was increased to 75 mm the light transmittance decreased to <50%. When the light detector was put on the opposite side of the nanocellulose paper from the incident beam, it could detect the transmitted beam at different angles from the incident beam. When the light detector was put on the same side of the nanocellulose paper with the incident beam, it could similarly detect the reflected beam at angles that differed from the incident beam. These results collectively indicate that although scattering is reduced compared with regular paper it nonetheless still exists in the nanocellulose paper. Nogi *et al.* found that polishing increases the transparency and flexibility of nanocellulose paper.<sup>66</sup> Henriksson *et al.* used different molar mass nanocelluloses to form nanocellulose papers and found that the highest molar mass MFCs resulted in the highest tensile strength (214 MPa) and strain-to-failure (10.1%).<sup>56</sup> *In situ* polymerization of MFCs with polypyrrole in the hydrogel gave rise to highly porous composites with a surface area of 90  $\text{m}^2 \text{ g}^{-1}$ . The polypyrrole coating in the hydrogel prevented the collapse of the MFC structure and the composite paper showed good electronic conductivity and ion-exchange capacity.<sup>67</sup> This composite material has been successfully used as an electrochemically controlled three-dimensional solid phase extraction material.<sup>68</sup>

In addition to MFCs, BC is an alternative starting material for nanocellulose paper production (Fig. 2).<sup>33</sup> When produced, BC naturally forms membranes, so the filtration step can be omitted<sup>69</sup> and BC papers can be obtained by simply pressing the BC hydrogel. BC papers produced at 2 MPa and 393 K were 60  $\mu\text{m}$  thick and exhibited cavities that were collectively one-third of its volume.<sup>70</sup> BC based nanocomposites can then be created by infiltrating a liquid resin or dissolved polymer (*e.g.*, epoxy) into these cavities. The mechanical strength of the nanocomposite paper was significantly increased due to the reinforcement of BC, while the transparency remained roughly the same.<sup>70</sup> Importantly, the transparency of the resin/BC composite papers is independent of the refractive index of the resins and the temperature.<sup>71</sup> Lee *et al.* manufactured BC and MFC papers by vacuum

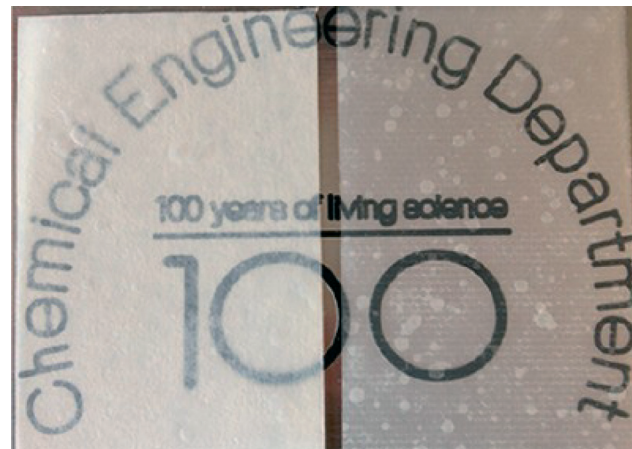


Fig. 2 Comparison of the transparent papers made from BC (left) and MFC (right).<sup>33</sup> Reprinted with permission from K. Y. Lee, T. Tammelin, K. Schulter, H. Kiiskinen, J. Samela, A. Bismarck, High performance cellulose nanocomposites: comparing the reinforcing ability of bacterial cellulose and nanofibrillated cellulose, *ACS Appl. Mater. Interfaces*, 2012, 4(8), 4078–4086. Copyright 2014 American Chemical Society.

filtration of nanocellulose suspensions followed by application of high pressure. Paper-epoxy composites were then prepared by vacuum assisted resin infusion. The final composites showed significantly higher mechanical strength than the epoxy.<sup>33</sup>

Translucent nanocellulose films with a thickness of 3–100  $\mu\text{m}$  were obtained from an aqueous suspension of MFCs. The suspension was spread on a plastic plate by a film applicator and dried at room temperature for 24 h. The biodegradable films obtained by this approach showed better tensile strength than print paper.<sup>1</sup> Microfibrils of 3–5 nm diameter were reconstituted into a thin film of 1.5–2.0  $\mu\text{m}$  thickness by simple solvent evaporation. The film showed an interesting ribbon structure where “receptors” such as polycationic poly-(diallyldimethylammoniumchloride) could be embedded in a sandwich structure to provide selective binding sites for the accumulation and transport of multiple charged or hydrophobic anions.<sup>72</sup> These nanocellulose films have been reinforced with  $\text{CaCO}_3$  and montmorillonite. Gebauer *et al.* first mixed nanocellulose with calcium chloride in aqueous solution and then transferred the mixture to an ethanol solution containing sodium carbonate. Because of the low solubility of calcium carbonate in ethanol, abrupt supersaturation led to a nucleation burst and calcium carbonate nanoparticles with a diameter of 11.3 nm formed on the nanocellulose surface. The composite film obtained this way was transparent and showed excellent mechanical strength.<sup>8</sup> Wu *et al.* prepared a transparent nanocellulose film by mixing and drying a TEMPO-oxidized nanocellulose and montmorillonite nanoplatelet dispersion. The resultant composite film showed a tensile strength of 509 MPa and the capacity to resist oxygen permeability.<sup>73</sup> Solid films prepared using cellulose whiskers preserve their liquid crystalline order and parabolic focal conic defects were found on the solid films.<sup>74</sup>



# Nanocellulose-based nanocomposites

Nanocellulose is an ideal platform to house a range of guest nanomaterials due to its high specific surface area, highly porous structure, and its mechanical strength. Nanocellulose-based nanocomposites combine the advantages of both the guest nanomaterial and the nanocellulose substrate and often exhibit synergistic properties. Guest nanomaterials can be incorporated into the nanocellulose substrate *via* three different approaches: 1) direct addition or formation of the guest nanomaterial in a nanocellulose dispersion; 2) formation of the guest nanomaterial in the bulk structure of nanocellulose-based materials such as BC membranes; 3) direct coating of the guest nanomaterial onto the nanocellulose surface as a nano-sized layer. A range of different guest nanomaterials such as metal NPs (Au, Ag, Pd, Ni, TiO<sub>2</sub>, CuO), mineral nanomaterials (CaCO<sub>3</sub>, SiO<sub>2</sub>, montmorillonite), and carbonaceous nanomaterials (carbon nanotube, graphene) have been incorporated into or onto nanocellulose substrates. When describing nanocellulose nanocomposite applications, we focus on their potential environmental applications (*e.g.*, antibacterial, catalytic, sensing, and energy). Nanocellulose

nanocomposite applications for medical devices, structural reinforcement and Li-ion battery manufacturing have been summarized previously and we refer the reader elsewhere for such information.<sup>35,47,75-77</sup> All the nanocellulose-based nanocomposites discussed *vide infra* are listed in Table 1.

## Antimicrobial filters

Electrospun nanofibrous filters have shown better performance (higher filtration efficiency and lower pressure drop) in air and drinking water purification compared to conventional polymer filters.<sup>18</sup> In some of the latest research, nanocellulose filters have shown the capacity to remove virus from water at levels that match the best industrial virus filters.<sup>20</sup> One of the biggest challenges for the application of filter membranes in water treatment is surface biofouling. The addition of antimicrobial materials such as AgNPs to the filter membrane can inhibit biofilm growth and prolong filter life. Chitosan-based antimicrobial materials have been proposed for both drinking water purification and storage.<sup>97,98</sup> Compared with bulk cellulose or other polymers, nanocelluloses possess the capacity to house greater numbers of AgNPs in a more homogeneous state due to their much higher surface to volume ratio, which then endows them with

**Table 1** Summary of nanocellulose-based nanocomposites

Nanocellulose type	Inorganic phase	Application	Functionalization technique	Precursor	References
MFCs	AgNPs	Antibacterial	UV radiation	AgNO <sub>3</sub>	78
MFCs	Titania, chitosan and AgNPs	Antibacterial	UV radiation	AgNO <sub>3</sub>	79
MFCs	AgNPs	Antibacterial	Adsorption	AgNPs	80
BC	AgNPs	Antibacterial	Hydrolytic decomposition/reduction by TEA	AgNO <sub>3</sub>	81
BC	AgNPs	Antibacterial	Reduction by NaBH <sub>4</sub>	AgNO <sub>3</sub>	82
BC	AgNPs	Antibacterial	Reduction by hydroxyls	AgNO <sub>3</sub>	83
BC	AgNPs	Antibacterial	Reduction by NH <sub>2</sub> NH <sub>2</sub> , NH <sub>2</sub> OH or C <sub>6</sub> H <sub>8</sub> O <sub>6</sub>	AgNO <sub>3</sub>	84
BC	AgCl NPs	Antibacterial	Precipitation	AgNO <sub>3</sub> /NaCl	85
MFCs	TiO <sub>2</sub> NPs	Catalytic	Mixing in dispersion	TiO <sub>2</sub> NPs	86
MFCs	TiO <sub>2</sub> thin layer	Catalytic/absorbent	CVD	Titanium isopropoxide	22 and 24
NCC	PdNPs	Catalytic	Reduction by H <sub>2</sub>	PdCl <sub>2</sub>	87
MFCs	AuNPs	Catalytic	Reduction by NaBH <sub>4</sub>	HAuCl <sub>4</sub>	88
NCC	AuNPs	Catalytic	Reduction by hydroxyls	HAuCl <sub>4</sub>	21
MFCs	Au-Pd bimetallic NPs	Catalytic	Reduction by NaBH <sub>4</sub>	HAuCl <sub>4</sub> /[Pd(NH <sub>3</sub> ) <sub>4</sub> ]Cl <sub>2</sub>	89
NCC	CuO NPs	Catalytic	Reduction by NaBH <sub>4</sub>	CuSO <sub>4</sub>	23
NCC	Pt, Cu, Ag, AuNPs	Catalytic/antibacterial/sensing	CTAB stabilization/reduction by NaBH <sub>4</sub>	K <sub>2</sub> PtCl <sub>6</sub> /CuCl <sub>2</sub> /AgNO <sub>3</sub> /HAuCl <sub>4</sub>	90
BC	AuNPs	Sensing	Reduction by PEI	HAuCl <sub>4</sub>	25, 27 and 91
BC	AuNPs	Sensing	Reduction by hydroxyls	HAuCl <sub>4</sub>	26
BC	AgNPs	Sensing	Reduction by sodium citrate	AgNO <sub>3</sub>	92
BC	Au-SiO <sub>2</sub> NPs	Sensing	Reduction by sodium citrate	HAuCl <sub>4</sub> /TEOS	93
NCC	AuNPs	Enzyme immobilization/sensing	Reduction by NaBH <sub>4</sub>	HAuCl <sub>4</sub>	94
BC	PdNPs	Fuel cell	Reduction by hydroxyls	Ammonium hexachloropalladate	28
MFCs	Tin-doped indium oxide thin layer	Solar cell	Radio frequency magnetron sputtering	In <sub>2</sub> O <sub>3</sub> /SnO <sub>2</sub>	65
MFCs	Graphite	Li-ion battery	Drying the slurry	Graphite	95
MFCs	Si thin layer and CNT	Li-ion battery	Plasma-enhanced CVD	CNT/Si	29
MFCs	Graphite, SiO <sub>2</sub> , LiFePO <sub>4</sub>	Li-ion battery	Suspension filtration and drying	Graphite/SiO <sub>2</sub> /LiFePO <sub>4</sub>	96



superior antimicrobial properties.<sup>79</sup> Moreover, the properly modified nanocellulose surface has improved capacity to immobilize AgNPs, which reduces the potential risks of AgNP leakage.<sup>78</sup> In this section, we describe recent literature examining the preparation of antimicrobial nanocellulose-based nanocomposites. Although not explicitly mentioned in many of these references, we believe these novel nanomaterials have promising applications as antimicrobial filters in drinking water purification if their porous structure is designed appropriately to meet this purpose.

Antimicrobial nanocellulose nanocomposites generally rely upon incorporation of silver based NPs into or on the nanocellulose matrix. Reduction of Ag<sup>+</sup> in the presence of nanocellulose is the most common way to synthesize AgNP/nanocellulose nanocomposites. The reduction methods include UV irradiation, addition of reducing chemicals (e.g., NaBH<sub>4</sub>), and *in situ* reduction by the nanocellulose hydroxyl groups. Here we introduce the nanocomposites obtained by different Ag<sup>+</sup> reduction methods and their antimicrobial activity.<sup>78,79,81</sup> AgNP decorated MFC films, hydrogels, and aerogels can be readily prepared by UV reduction of Ag<sup>+</sup> in the corresponding matrix.<sup>78</sup> In one instance, Ag<sup>+</sup> addition facilitated MFC gelation and a gel-like hydrogel was formed rapidly. The rapid gelation was attributed to complexation between the carboxylate groups of the MFCs and Ag<sup>+</sup> and hydrogen bonding between the hydroxyl groups of the MFCs. The method used to dry the hydrogel will determine its final form. If the hydrogel is dried in a ventilated oven purged with nitrogen a transparent film can be formed. In contrast, if the hydrogel is freeze-dried a sponge-like aerogel is formed. TEM results indicated that AgNPs with a uniform diameter of  $\approx 2$  nm formed following UV exposure.<sup>78</sup> This AgNP/MFC nanocomposite can inhibit the growth of *Escherichia coli* and *Staphylococcus aureus* whereas the MFC didn't show any inhibition effects. Xiao *et al.* also used UV irradiation for the fabrication of AgNP/nanocellulose nanocomposites.<sup>79</sup> But instead of directly mixing Ag<sup>+</sup> and nanocellulose, they first functionalized their MFCs with titania and chitosan through layer by layer self-assembly. A large amount of Ag<sup>+</sup> could be adsorbed on the surface of the chitosan nanofilms because of the chelating capability of chitosan. Following application of UV irradiation, AgNPs with diameter of 4–20 nm were homogeneously dispersed across the film surface. This nanocomposite has an Ag content as high as 1.25% by weight that endows it with superior antimicrobial properties.<sup>79</sup>

In addition to UV irradiation, the application of reducing agents is an alternative way to reduce Ag<sup>+</sup> to AgNPs. Barud *et al.* incorporated AgNPs on BC membranes by reduction of AgNO<sub>3</sub> in the presence of triethanolamine (TEA).<sup>81</sup> This work suggested that TEA acted as both reducing and chelating agent, influencing Ag nucleation and growth. The AgNP/BC nanocomposites displayed strong antimicrobial activity towards *S. aureus*, *P. aeruginosa*, and *E. coli*.<sup>81</sup> Yang *et al.* incorporated AgNPs on BC membrane by reduction of AgNO<sub>3</sub> in the presence of NaBH<sub>4</sub>. The size and size

distribution of AgNPs formed in BC were analyzed by means of transmission electron microscopy (TEM) and Image J software. The average size of AgNPs in maltose, glucose, and sucrose-derived BC were  $8.3 \pm 3.6$  nm,  $9.8 \pm 3.7$  nm, and  $7.9 \pm 3.8$  nm. The hydroxyl groups were found to be anchors of Ag<sup>+</sup> and the nanosized pores of BC served as reactors for the formation of small and narrowly distributed AgNPs.<sup>82</sup> Instead of using UV light or reducing reagents, Ag<sup>+</sup> can also be reduced by the hydroxyl groups on BC at elevated temperature (353 K). The morphology of the nanocomposites was characterized with SEM and the AgNP size distribution was obtained using Image J software. It was observed that AgNPs were homogeneously dispersed in the BC matrix and showed a narrow size distribution with an average size of  $17.1 \pm 5.9$  nm. The AgNP/BC nanocomposites produced by this technique inhibited the growth of *S. aureus* for 72 h and thus have potential for many antimicrobial applications.<sup>83</sup>

In the previous paragraphs, we introduced the preparation of antimicrobial AgNP/nanocellulose nanocomposites. In addition to incorporating AgNPs, AgCl-NPs and Ag nanoclusters (AgNCs) have also been impregnated into nanocellulose matrices for antimicrobial purposes.<sup>80,85</sup> AgCl NPs were synthesized in a BC matrix by soaking BC in 1 mM AgNO<sub>3</sub> solution and then applying 1 mM NaCl solutions sequentially for 10 cycles. The AgCl NP/BC nanocomposites produced by this approach showed strong antimicrobial activity against both *E. coli* and *S. aureus*.<sup>85</sup> Díez *et al.* described a simple method for Ag nanocluster/nanocellulose nanocomposite synthesis. Ag nanoclusters (AgNCs; diameter  $< 2$  nm) could be adsorbed on the nanocellulose films by immersing them in aqueous AgNC suspensions and then agitating the suspensions in the dark. AgNCs show higher fluorescence activity than AgNPs because of electronic transitions between quantized energy levels.<sup>99</sup> The nanocomposites obtained by this approach showed both fluorescence activity as well as antimicrobial activity.<sup>80</sup> Based upon the literature summarized herein, we know that silver-based NP/nanocellulose nanocomposites can be easily synthesized by either reduction of Ag<sup>+</sup> or by soaking nanocellulose in Ag-based nanoparticle suspensions. Because these antimicrobial nanocomposites show great promise for use in wound dressing, antimicrobial film preparations or as antimicrobial filters we anticipate that research further examining their capabilities will be of growing research focus.

## Catalysis

Water pollutant remediation by catalytic decomposition of organic pollutants is a growing application of nanocellulose-based nanocomposites.<sup>21–23,86–90</sup> There are mainly two categories of guest NPs used for catalytic applications: 1) photocatalysts such as TiO<sub>2</sub> and 2) precious metals (Au, Ag, Pt, *etc.*). When used for catalysis, nanocellulose typically acts as a catalyst support to hinder nanoparticle aggregation. In this section we introduce TiO<sub>2</sub>/nanocellulose nanocomposites first and then discuss precious metal/nanocellulose nanocomposites.



Hard and transparent films can be formed by mixing MFCs with  $\text{TiO}_2$ -NPs. As shown by FTIR,  $\text{TiO}_2$ -NPs interact with the MFC surface through electrostatic interactions. With an increase in  $\text{TiO}_2$  content, the transparency and the mechanical strength of the nanocomposite decreases.<sup>86</sup> Although not explicitly discussed in this reference, it is our opinion that this nanocomposite could be used for photocatalytic decomposition of organic pollutants. Evidence to support this hypothesis is prevalent in the literature. For example, a 7 nm wide  $\text{TiO}_2$  layer was coated onto a nanocellulose aerogel *via* chemical vapor deposition. Methylene blue, used as a model contaminant, was then efficiently decomposed on the nanocomposite under UV illumination, thus indicating the materials' potential use for water treatment applications.<sup>22</sup> In addition to its catalytic advantages, this  $\text{TiO}_2$ /nanocellulose nanocomposite showed interesting photoswitchable water superabsorption. The  $\text{TiO}_2$  coated cellulose aerogel is hydrophobic with a water contact angle of 140°. Following UV light illumination, the nanocomposite became super hydrophilic. The sample then regained its hydrophobicity upon storage in the dark.<sup>22</sup> Due to the super light and hydrophobic nature of the  $\text{TiO}_2$  coated MFC aerogel, it was able to float on water and absorb different organic solvents at levels as high as 20–40× its own weight, thus indicating it can be used as an absorbent for spilt oil removal from water.<sup>24</sup>

In addition to  $\text{TiO}_2$ , precious metals (Au, Ag, Pt, and Pd) are also commonly used as catalysts. Metal-NP/nanocellulose nanocomposites are often produced by reduction of metal salts in the presence of nanocellulose. The reduction agents include a variety of chemicals such as  $\text{H}_2$ ,  $\text{NaBH}_4$ , and  $\text{Na}_3\text{citrate}$  or the hydroxyl groups of the nanocellulose. Cirtiu *et al.* exposed a suspension of  $\text{PdCl}_2$  and NCC to  $\text{H}_2$  pressure (4 bar) for 2 h.  $\text{Pd}^{2+}$  was reduced to PdNPs that have an average particle size of  $3.6 \pm 0.8$  nm. Phenol was efficiently converted to cyclohexanone *via* catalytic hydrogenation over this PdNP/NCC nanocomposite. This reaction did not occur when the PdNPs were synthesized in the absence of NCC. This result was attributed to the aggregation of the PdNPs, and the resultant loss in reactive surface area, in the absence of the NCC support.<sup>87</sup> Similarly, TEMPO oxidized MFCs were used to support production of dispersed AuNPs. In this synthesis, MFC surface associated  $\text{Au}^{3+}$  was reduced by  $\text{NaBH}_4$  at room temperature to produce highly dispersed AuNPs. TEM and selected area electron diffraction results showed that well dispersed crystalline AuNPs with a uniform diameter of 5 nm formed along the fibers. Compared with the AuNP/cellulose composite and AuNP solution, the AuNP/MFC nanocomposite has a narrower UV-vis absorption spectrum, indicating it contains less AuNP aggregates. The author speculated that the carboxylate groups of MFC act to stabilize AuNPs and avoid the formation of large AuNP aggregates. The AuNP/MFC nanocomposites showed excellent catalytic performance for the degradation of 4-nitrophenol. Nitroaromatic compounds are toxic organic byproducts produced during the manufacturing process of agrochemicals, dyes

and pharmaceuticals.<sup>23</sup> As such, 4-nitrophenol is often used as a model compound to evaluate the catalytic performance of metal NPs.<sup>21,23,88</sup> The turnover frequency of the AuNP/MFC nanocomposites was  $840\times$  greater than that of conventional AuNP/polymer composites.<sup>88</sup> Wu *et al.* proposed a green method for the synthesis of AuNP/NCC nanocomposites. In this room temperature synthesis,  $\text{Au}^{3+}$  was reduced *in situ* by the hydroxyl groups of NCC to produce AuNPs with an average diameter of 30 nm. According to the TEM results the AuNPs were sparsely distributed and did not grow along the NCC fibers. The AuNP/NCC nanocomposites obtained are 3× more efficient than unsupported AuNPs for the catalytic degradation of 4-nitrophenol which is also due to the enhanced dispersion of the AuNPs.<sup>21</sup>

Azetsu *et al.* explored the catalytic activity of Au and Pd bimetallic NPs using TEMPO-oxidized cellulose MFCs as support. Highly dispersed Au, Pd, and hybrid Au–Pd NP catalysts were successfully synthesized *in situ* onto the surface of MFCs due to the high density of carboxylate groups present in the MFCs (1.0 wt%,  $\text{COOH}^-$  0.96 mmol g<sup>-1</sup>).  $\text{NaBH}_4$  was used as the reducing agent and the carboxylate groups acted as AuNP anchors. The different NP/MFC nanocomposites were compared in terms of catalytic behavior for the reduction of 4-nitrophenol to 4-aminophenol. The turnover frequency for the reduction-catalyzed reaction was measured from the variation in absorbance at 400 nm. It was found that 4 nm AuNPs deposited onto MFCs had a higher catalytic activity than when they were deposited onto other synthetic and natural polymeric substrates. However, a much higher catalytic efficiency in the reduction of 4-nitrophenol was observed for the hybrid Au–Pd NP/MFC nanocomposite with a 3:1 ratio of Au:Pd. It was hypothesized that the enhancement in catalytic efficiency might be attributed to electronic mediated ligand effects. These so-called electronic mediated ligand effects are the acceleration of catalytic reactions induced by electronic interactions between two metal NPs relative to the mono metal NPs.<sup>89</sup>

In addition to  $\text{TiO}_2$  and precious metal NPs, CuO-NPs can also be used as catalysts. Catalytic degradation of 4-nitrophenol was performed using CuO-NP/NCC as catalysts.  $\text{Cu}^{2+}$  was reduced by  $\text{NaBH}_4$  at ambient condition and CuO-NPs were formed on the surface of NCC. The CuO-NP/NCC nanocomposites showed a better performance for 4-nitrophenol decomposition than unsupported and graphene supported CuO-NPs because of the higher surface area of NCC and the immobilization of CuO-NPs by the hydroxyl groups of NCC.<sup>23</sup> In all the studies previously discussed in this section, the metal NPs were thought to be randomly deposited on the porous NCC matrix and the surface coverage of NPs on NCC was low. To increase the surface coverage of metal NPs on NCC, Padalkar *et al.* proposed the use of cetyltrimethylammonium bromide (CTAB) in the synthesis process. Through its cationic quaternary ammonium groups CTAB adsorbed to the metal NP surface can interact with electron-rich hydroxyl groups and anionic charged groups on the NCC surface. The metal NPs synthesized in the absence



of CTAB tended to form on the TEM grid substrate instead of the NCC surface (Fig. 3a) while the metal NPs synthesized in the presence of CTAB formed along the fibrils (Fig. 3b).<sup>90</sup>

### Pollutant sensors

AuNP/nanocellulose nanocomposites, employed as biosensors, have been developed by many researchers.<sup>25–27,91,93</sup> Some of these studies took advantage of the conductivity of AuNP and the biocompatibility of BC by integrating the nanocomposite into an electrode to detect chemicals electrochemically.<sup>25,27,91</sup> Zhang *et al.* synthesized AuNP/BC nanocomposites and used them as sensors for  $H_2O_2$  and glucose detection.<sup>27</sup> First, the BC hydrogels were dispersed in water by ultrasonication and then  $HAuCl_4$  and polyethylenimine (PEI) were added to the dispersion. The mixture was incubated at 60 °C and AuNPs formed on the surface of the nanocellulose with PEI as both linking and reducing agent. Adding different halides into the mixture alters the gold shell on the nanocellulose surface. According to the SEM results, chloride addition will lead to a uniform and smooth AuNP coating on the BC surface with a AuNP diameter of 9 nm. Bromide addition leads to larger AuNP agglomerates and higher AuNP coverage on the BC surface. Iodide addition leads to submicrometer-sized AuNPs and low AuNP coverage on BC surface. The resultant AuNP/BC nanocomposites were coated onto a glassy carbon electrode (GCE) and then functionalized with horseradish peroxidase (HRP), hemoglobin (HB) and myoglobin (MB). The as-obtained AuNP/BC/HRP/GCE, AuNP/BC/HB/GCE and AuNP/BC/MB/GCE were found to be efficient sensors for  $H_2O_2$  with AuNP/BC/HRP/GCE having the best response.<sup>25,27</sup> Meanwhile the AuNP/BC/GCE composite following functionalization with two enzymes – HRP and glucose oxidase ( $GO_x$ ), was found to be an efficient sensor for glucose.<sup>91</sup>

Surface-enhanced Raman spectroscopy (SERS) of AuNPs and AgNPs has been extensively studied.<sup>100–103</sup> The biosensors developed based on this technique have been applied in the monitoring of waterborne pathogens and organic contaminants. For example, in one previous study from our

group, two notorious waterborne protozoa – *Cryptosporidium parvum* and *Giardia lamblia* have been detected using an immunogold-based biosensor. It is often inconvenient to use AuNP/AgNP colloids directly in real-world applications. To overcome this problem, a flexible SERS substrate such as paper is desirable. Nanocellulose can form papers or films that can house SERS-active NPs; however, the performance of AuNP/nanocellulose or AgNP/nanocellulose nanocomposites as SERS substrates has to date only been demonstrated by a few studies.<sup>26,92</sup> Marques *et al.* synthesized an AgNP/BC nanocomposite through *in situ* reduction of  $Ag^+$  by  $Na_3citrate$  on the BC matrix. The resulting AgNP/BC substrate can detect thiosalicylic acid and 2,2'-dithiodipyridine at concentrations as low as  $10^{-4}$  M. In addition, the SERS spectra of three amino acids – L-phenylalanine, L-glutamin, and L-histidine have been obtained with this substrate.<sup>92</sup> Park *et al.* synthesized AuNP/BC nanocomposites as substrates for SERS detection of trace organic chemicals – 4-fluorobenzenethiol (4-FBT) and phenylacetic acid (PAA). For this application,  $HAuCl_4$  was reduced *in situ* by the hydroxyl groups of BC at 373 K to form AuNPs in the interstitial space of the layer-structured BC hydrogel. When the hydrogel dried, the distance between the adjacent layers of the hydrogel and the attached AuNPs significantly decreased, thus creating SERS hot spots (Fig. 4). Using this approach, low concentrations of PAA ( $10^{-7}$  M) were detected. Interestingly, for 4-FBT, which has high affinity to AuNPs, the minimum concentration detected was considerably higher ( $10^{-5}$  M). This approach took advantage of the three dimensional structure of BC. Compared with traditional two-dimensional SERS substrates, drying mediated deformation of the three dimensional AuNP/BC nanocomposites created hot spots in the vertical direction resulting in much higher Raman signals.<sup>26</sup>

Instead of being directly used in the biosensor, AuNPs can also be functionalized to achieve additional goals. Pinto *et al.* deposited AuNPs onto BC by reducing an  $Au^{3+}$ -BC complex with  $Na_3citrate$ . To generate a specific separation between AuNPs, a homogeneous coating of  $SiO_2$  on the AuNPs was developed. By this approach they were able to vary the thickness of the  $SiO_2$  shell on the AuNPs from 15 to

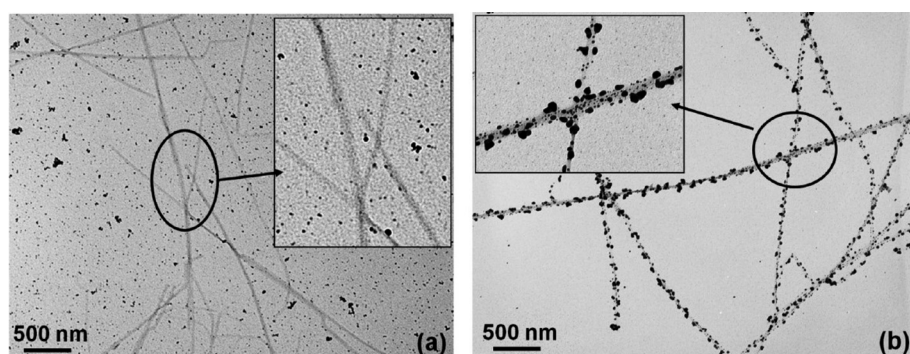
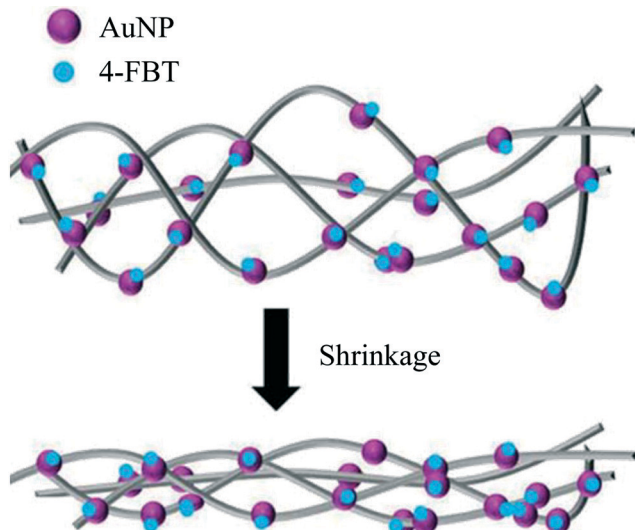


Fig. 3 TEM images of the AgNPs synthesis on tunicate NCC without CTAB (a) and with CTAB (b).<sup>90</sup> Reprinted with permission from S. Padalkar, J. Capadona, S. J. Rowan, C. Weder, Y. H. Won, L. A. Stanciu, R. J. Moon, *Natural biopolymers: novel templates for the synthesis of nanostructures*, *Langmuir*, 2010, 26(11), 8497–8502. Copyright 2014 American Chemical Society.





**Fig. 4** The schematic description of for the detection of 4-FBT by deformation of the AuNP/BC hydrogel.<sup>26</sup> Reprinted with permission from M. Park, H. Chang, D. H. Jeong, J. Hyun, Spatial deformation of nanocellulose hydrogel enhances SERS, *BioChip J.*, 2013, 7(3), 234–241. Copyright 2014 The Korean BioChip Society and Springer-Verlag Berlin Heidelberg.

100 nm, which could be observed in TEM images. The BC membranes functionalized with AuNPs or Au-SiO<sub>2</sub> NPs were then assembled using layer-by-layer (LbL) deposition using poly(diallyldimethylammonium chloride), PDDA, and poly(sodium 4-styrenesulfonate), PSS. This work suggested that it could be possible to modify the optical properties of the AuNP/BC nanocomposites by coating the AuNPs with SiO<sub>2</sub> or by alternating the composition of the assembled layers with AuNP/BC and Au-SiO<sub>2</sub> NP/BC membranes. A suitable application of this nanocomposite is a paper-based core–shell biosensor where long term optical and chemical stability are important.<sup>93</sup> AuNP/NCC nanocomposites have also been used as a platform for enzyme immobilization. First, AuNPs were formed on the surface of NCC by the reduction of HAuCl<sub>4</sub> by NaBH<sub>4</sub>. Then thioctic acid (Thc) containing both –SH and –COOH was bound to the AuNP surface and its carboxylic acid groups were activated by 1-ethyl-3-[3-(dimethylamino)propyl]carbodiimide (EDC) and N-hydroxysulfosuccinimide (NHS). Finally, the amino groups of the enzyme – cyclodextrin glycosyl transferase (CGTase) were covalently bound to the activated carboxylic acid groups on the nanocomposites. The binding capacity of CGTase on the AuNP/NCC nanocomposites was 165 mg g<sup>-1</sup> of NCC and the CGTase on the matrix still showed significant biocatalytic activity.<sup>94</sup> The high loading of enzymes on this nanocomposite suggests that it can be used for the fabrication of enzyme-based biosensors.

### Energy applications

Nanocellulose-based nanocomposites can also be applied in fuel cell, solar cell and Li-ion battery manufacturing. Fuel

cells are devices that can convert chemical energy to electricity. Fuel (usually H<sub>2</sub>) is catalytically oxidized at the anode and O<sub>2</sub> at the cathode is catalytically reduced to H<sub>2</sub>O. Electrons flow from anode to cathode through an external circuit. BC has been found to be a good substrate to host a large number of nano-sized anode catalysts. When a BC membrane was soaked in a 5 mM solution of ammonium hexachloropalladate, PdNPs were precipitated in the BC membrane. However, the incubation of plant cellulose in hexachloropalladate solution did not result in precipitation. Tapping mode AFM showed that the plant cellulose possessed a tightly woven and ordered fibrous structure, while the BC fibers were organized into tunnels and were much looser. Accordingly, the precipitation of PdNPs in BC was attributed to the accessibility of reducing groups within their looser structure. A native BC membrane sandwiched between PdNP/BC nanocomposites was used as a membrane electrode assembly (MEA) in a fuel cell. The thickness of the MEA was 150 µm and the density of palladium in the anode and cathode membranes was 0.4 mg cm<sup>-2</sup> membrane (dry weight). H<sub>2</sub> applied to the PdNP/BC anode was oxidized and a maximum current of about 0.26 mA was detected, thus indicating this nanocomposite has the potential to be applied in energy conversion devices. This PdNP/BC membrane shows advantages over other polyelectrolyte membranes due to its higher thermal stability and lower gas crossover.<sup>28</sup>

Solar cells are devices that can convert solar energy to electricity. Since nanocellulose paper is transparent, smooth, and mechanically strong, it is a promising candidate to be used as a solar cell substrate. Hu *et al.* designed a solar cell based on a transparent nanocellulose paper (Fig. 5a). In detail, an indium tin oxide (ITO) film was coated on nanocellulose paper by radio frequency magnetron sputtering of a target composed of 90% In<sub>2</sub>O<sub>3</sub> and 10% SnO<sub>2</sub>. After coating, the originally transparent paper became translucent. Then the ITO-coated nanocellulose paper was treated with poly(3-hexylthiophene) (P3HT) and [6:6]-phenyl-C<sub>61</sub>-butyric acid methyl ester (PCBM) as the light absorbing layer. The transparent nanopaper increased the path length of light through the absorbing layer, thus resulting in greater solar light absorption. The solar cell as-prepared showed a power conversion efficiency of 0.4%, which illustrates the opportunity to apply nanocellulose paper for photovoltaic applications.<sup>65</sup> However, because the sheet resistance of ITO on nanopaper is 50–100 times higher than that on glass, the short-circuit current J<sub>sc</sub> and overall power conversion efficiency (PCE) of the nanopaper-based solar cell were lower than the glass-based solar cell (Fig. 5b).

In addition to fuel cells and solar cells, nanocellulose can also be used in Li-ion batteries (LIBs). LIBs are popular rechargeable energy storage devices that are widely used in consumer electronic products. Nanocellulose paper provides an opportunity to design thin, flexible and high-performance LIBs. Cellulose based LIBs have been well summarized in a recent review paper by Jabbour *et al.*<sup>76</sup> Here we focus on nanocellulose based LIBs and their advantages. Nanocelluloses



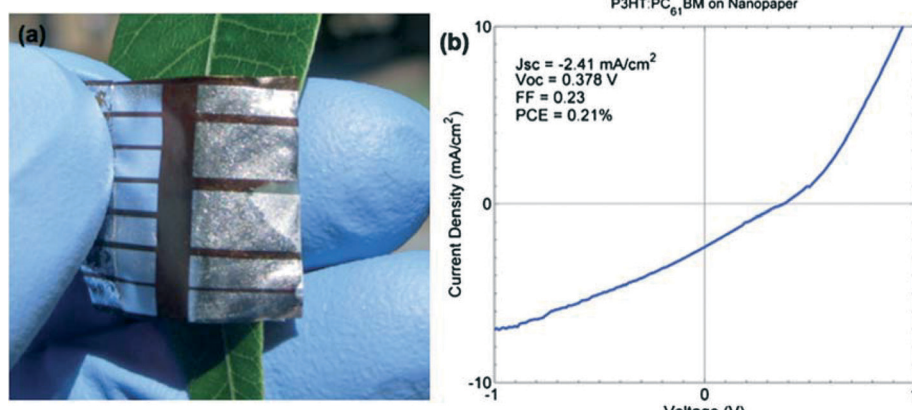


**Fig. 5** Printed solar cells on transparent and conductive nanopaper. (a) An organic solar cell on conductive nanopaper. (b) The  $I$ - $V$  curve of the organic solar cell shown in (a).<sup>65</sup> Reproduced from L. Hu, G. Zheng, J. Yao, N. Liu, B. Weil, M. Eskilsson, E. Karabulut, Z. Ruan, S. Fan, J. T. Bloking, Transparent and conductive paper from nanocellulose fibers, *Energy Environ. Sci.*, 2013, **6**(2), 513–518. With permission from The Royal Society of Chemistry. Copyright 2014 The Royal Society of Chemistry.

used as electrode, separator and electrolyte in LIB cells have been reported.<sup>29,67,96,104–106</sup> Jabbour *et al.* developed a flexible graphite/MFC LIB anode by vacuum drying a graphite/MFC slurry at 313 K overnight. In addition to the graphite/MFC anode, the cell also contained Li foil cathode and LiPF<sub>6</sub> in ethylene carbonate and diethyl carbonate as electrolyte. The graphite/MFC anode showed similar charge/discharge capacity as commonly used graphite/poly(vinylidene fluoride) (PVdF) and good stability, thus indicating sustainable MFCs can replace the synthetic chemical PVdF for LIB anode manufacturing.<sup>95</sup> Hu *et al.* developed a Si-coated CNT/nanocellulose paper (Si-nanopaper) used as the LIB electrode. First, the CNT/nanocellulose paper was prepared by freeze drying the homogeneously mixed CNT/nanocellulose hydrogel. The addition of CNT imparts the nanocomposite with high electrical conductivity. Secondly, a thin layer of Si was coated on the CNT/nanocellulose paper by a plasma-enhanced CVD (PECVD) method. Finally, the cell was built with Si-nanopaper, Li metal foil and a Celgard 2250 separator soaked in electrolyte (LiPF<sub>6</sub> in ethylene carbonate/diethyl carbonate). The Si-nanopaper obtained showed a stable capacity of 1200 mA h g<sup>-1</sup> after 100 charge/discharge cycles, a value which is more than 3 $\times$  the theoretical capacity of the commonly used graphite anode. The high stability of the Si-nanopaper can be attributed to the flexible and highly porous structure of the CNT/nanocellulose paper, which provides enough space for accommodation of the expanding volume of the Si layer during lithiation.<sup>29</sup> Leijonmarck *et al.* integrated the MFC based electrode and separator into a single paper so as to make a flexible LIB cell.<sup>96</sup> The cell was made by consecutively vacuum filtering the negative electrode suspension (MFCs + graphite), separator suspension (MFCs + SiO<sub>2</sub>) and positive electrode suspension (MFCs + LiFePO<sub>4</sub>) on a filter paper. The dried cell contains three layers stacked together with two electrodes outside and the separator in the middle. The flexible paper battery is strong and shows satisfactory charge/discharge cycle capacities. The MFCs here are

used as a binder and provide a strong and flexible skeleton for the LIB cell. Except for being used in electrode or separator, nanocellulose can also be used in electrolytes for reinforcement purposes. As stated previously, we do not discuss the reinforcement function of nanocellulose in this review and we refer readers to the other references for detailed information.<sup>104–106</sup>

## Conclusions and future research needs

In this review, we briefly discussed the recent progress made in the preparation of nanocellulose-based nanomaterials and their potential environmental applications. Nanocellulose has abundant sources and is relatively cheap. The top-down disintegration of cellulose pulp can produce ultrathin nanofibers with diameters of 2–5 nm. These nanocelluloses show extraordinary optical, mechanical, and thermal properties. Paper, film, fiber, and aerogel synthesized by the bottom-up assemblage of nanocellulose provide adequate space to serve as a strong carrier for the incorporation of guest nanomaterials. The nanocellulose-based nanocomposites showed many advantages, including antimicrobial and catalytic activities, which can be applied for water purification. AuNP impregnated nanocellulose may be an excellent SERS substrate if both of the loading and size of AuNPs can be increased. Nanocellulose has also been demonstrated as a novel substrate for fuel cell fabrication and thus shows promise in energy applications.

In the future, methods to better control the size and distribution of metal and other NPs in nanocellulose substrates as dictated by the ultimate application will be an interesting research topic. For catalytic applications, dispersed and small metal NPs are desirable, while for SERS applications, aggregated and large metal NPs are required. The loading of NPs is also quite important for the applications of the nanocomposites. The loading limit of different NPs in the

nanocellulose matrix is worth further exploration. The addition of inorganic materials into the nanocellulose matrix may alter their sustainability. Therefore, research efforts should be made to prolong the life of or regenerate those nanocomposites to make them truly sustainable. As more and more efforts have been paid to looking for a cheap and environment-friendly material to address emerging environmental problems, nanocellulose-based nanocomposites should be a competitive candidate.

## Acknowledgements

Funding for this study was provided by the US National Science Foundation (NSF; BES 1236005) and the Virginia Tech Institute for Critical Technology and Applied Science. Support for HW was provided by the Virginia Tech Graduate School through the Sustainable Nanotechnology Interdisciplinary Graduate Education Program (VTSuN IGEP). Additional funding was provided by NSF and the Environmental Protection Agency under NSF Cooperative Agreement EF-0830093, Center for the Environmental Implications of NanoTechnology (CEINT). Any opinions, findings, conclusions or recommendations expressed in this material are those of the authors and do not necessarily reflect the views of the NSF or the EPA. This work has not been subjected to EPA review and no official endorsement should be inferred.

## References

- 1 T. Taniguchi and K. Okamura, New films produced from microfibrillated natural fibres, *Polym. Int.*, 1998, **47**(3), 291–294.
- 2 H. Sehaqui, A. Liu, Q. Zhou and L. A. Berglund, Fast preparation procedure for large, flat cellulose and cellulose/inorganic nanopaper structures, *Biomacromolecules*, 2010, **11**(9), 2195–2198.
- 3 J. Cai, S. Liu, J. Feng, S. Kimura, M. Wada, S. Kuga and L. Zhang, Cellulose–silica nanocomposite aerogels by in situ formation of silica in cellulose gel, *Angew. Chem.*, 2012, **124**(9), 2118–2121.
- 4 Y. Shin, J. M. Blackwood, I. T. Bae, B. W. Arey and G. J. Exarhos, Synthesis and stabilization of selenium nanoparticles on cellulose nanocrystal, *Mater. Lett.*, 2007, **61**(21), 4297–4300.
- 5 Y. Shin, I. T. Bae, B. W. Arey and G. J. Exarhos, Simple preparation and stabilization of nickel nanocrystals on cellulose nanocrystal, *Mater. Lett.*, 2007, **61**(14), 3215–3217.
- 6 T. Vijayabaskaran and S. Vitta, Ni/Bacterial cellulose nanocomposite, a magnetically active inorganic-organic hybrid gel, *RSC Adv.*, 2013, **3**, 12765–12773.
- 7 M. Wang, I. V. Anoshkin, A. G. Nasibulin, J. T. Korhonen, J. Seitsonen, J. Pere, E. I. Kauppinen, R. H. Ras and O. Ikkala, Modifying native nanocellulose aerogels with carbon nanotubes for mechanoresponsive conductivity and pressure sensing, *Adv. Mater.*, 2013, **25**(17), 2428–2432.
- 8 D. Gebauer, V. Oliynyk, M. Salajkova, J. Sort, Q. Zhou, L. Bergström and G. Salazar-Alvarez, A transparent hybrid of nanocrystalline cellulose and amorphous calcium carbonate nanoparticles, *Nanoscale*, 2011, **3**(9), 3563–3566.
- 9 L. Melone, L. Altomare, I. Alfieri, A. Lorenzi, L. De Nardo and C. Punta, Ceramic aerogels from TEMPO-oxidized cellulose nanofibre templates: synthesis, characterization, and photocatalytic properties, *J. Photochem. Photobiol. A*, 2013, **261**, 53–60.
- 10 K. E. Shopsowitz, H. Qi, W. Y. Hamad and M. J. MacLachlan, Free-standing mesoporous silica films with tunable chiral nematic structures, *Nature*, 2010, **468**(7322), 422–425.
- 11 S. Rebouillat and F. Pla, State of the art manufacturing and engineering of nanocellulose: a review of available data and industrial applications, *J. Biomater. Nanobiotechnol.*, 2013, **4**(2), 165–188.
- 12 R. J. Moon, A. Martini, J. Nairn, J. Simonsen and J. Youngblood, Cellulose nanomaterials review: structure, properties and nanocomposites, *Chem. Soc. Rev.*, 2011, **40**(7), 3941–3994.
- 13 S. Eichhorn, A. Dufresne, M. Aranguren, N. Marcovich, J. Capadona, S. Rowan, C. Weder, W. Thielemans, M. Roman and S. Rennekar, Review: current international research into cellulose nanofibres and nanocomposites, *J. Mater. Sci.*, 2010, **45**(1), 1–33.
- 14 M. A. S. Azizi Samir, F. Alloin and A. Dufresne, Review of recent research into cellulosic whiskers, their properties and their application in nanocomposite field, *Biomacromolecules*, 2005, **6**(2), 612–626.
- 15 S. Vitta and V. Thiruvengadam, Multifunctional bacterial cellulose and nanoparticle-embedded composites, *Curr. Sci.*, 2012, **102**(10), 1398–1405.
- 16 B. Wicklein and G. Salazar-Alvarez, Functional hybrids based on biogenic nanofibrils and inorganic nanomaterials, *J. Mater. Chem. A*, 2013, **1**(18), 5469–5478.
- 17 E. Lam, K. B. Male, J. H. Chong, A. C. Leung and J. H. Luong, Applications of functionalized and nanoparticle-modified nanocrystalline cellulose, *Trends Biotechnol.*, 2012, **30**(5), 283–290.
- 18 K. Yoon, B. S. Hsiao and B. Chu, Functional nanofibers for environmental applications, *J. Mater. Chem.*, 2008, **18**(44), 5326–5334.
- 19 T. A. Dankovich and D. G. Gray, Bactericidal paper impregnated with silver nanoparticles for point-of-use water treatment, *Environ. Sci. Technol.*, 2011, **45**(5), 1992–1998.
- 20 G. Metreveli, L. Wågberg, E. Emmoth, S. Belák, M. Strømme and A. Mihranyan, A Size-exclusion nanocellulose filter paper for virus removal, *Adv. Healthcare Mater.*, 2014, DOI: 10.1002/adhm.201300641.
- 21 X. Wu, C. Lu, Z. Zhou, G. Yuan, R. Xiong and X. Zhang, Green synthesis and formation mechanism of cellulose nanocrystal-supported gold nanoparticles with enhanced catalytic performance, *Environ. Sci.: Nano*, 2014, **1**(1), 71–79.
- 22 M. Kettunen, R. J. Silvennoinen, N. Houbenov, A. Nykänen, J. Ruokolainen, J. Sainio, V. Pore, M. Kemell, M. Ankerfors



and T. Lindström, Photoswitchable superabsorbency based on nanocellulose aerogels, *Adv. Funct. Mater.*, 2011, **21**(3), 510–517.

23 Z. Zhou, C. Lu, X. Wu and X. Zhang, Cellulose nanocrystals as a novel support for CuO nanoparticles catalysts: facile synthesis and their application to 4-nitrophenol reduction, *RSC Adv.*, 2013, **3**(48), 26066–26073.

24 J. T. Korhonen, M. Kettunen, R. H. Ras and O. Ikkala, Hydrophobic nanocellulose aerogels as floating, sustainable, reusable, and recyclable oil absorbents, *ACS Appl. Mater. Interfaces*, 2011, **3**(6), 1813–1816.

25 W. Wang, T. J. Zhang, D. W. Zhang, H. Y. Li, Y. R. Ma, L. M. Qi, Y. L. Zhou and X. X. Zhang, Amperometric hydrogen peroxide biosensor based on the immobilization of heme proteins on gold nanoparticles–bacteria cellulose nanofibers nanocomposite, *Talanta*, 2011, **84**(1), 71–77.

26 M. Park, H. Chang, D. H. Jeong and J. Hyun, Spatial deformation of nanocellulose hydrogel enhances SERS, *BioChip J.*, 2013, **7**(3), 234–241.

27 T. Zhang, W. Wang, D. Zhang, X. Zhang, Y. Ma, Y. Zhou and L. Qi, Biotemplated synthesis of gold nanoparticle–bacteria cellulose nanofiber nanocomposites and their application in biosensing, *Adv. Funct. Mater.*, 2010, **20**(7), 1152–1160.

28 B. R. Evans, H. M. O'Neill, V. P. Malyvanh, I. Lee and J. Woodward, Palladium-bacterial cellulose membranes for fuel cells, *Biosens. Bioelectron.*, 2003, **18**(7), 917–923.

29 L. Hu, N. Liu, M. Eskilsson, G. Zheng, J. McDonough, L. Wågberg and Y. Cui, Silicon-conductive nanopaper for Li-ion batteries, *Nano Energy*, 2013, **2**(1), 138–145.

30 A. Nakagaito and H. Yano, The effect of morphological changes from pulp fiber towards nano-scale fibrillated cellulose on the mechanical properties of high-strength plant fiber based composites, *Appl. Phys. A: Mater. Sci. Process*, 2004, **78**(4), 547–552.

31 A. Dammak, C. Moreau, N. Beury, K. Schwikal, H. T. Winter, E. Bonnin, B. Saake and B. Cathala, Elaboration of multilayered thin films based on cellulose nanocrystals and cationic xylans: application to xylanase activity detection, *Holzforschung*, 2013, **67**(5), 579–586.

32 T. Saito, Y. Nishiyama, J. L. Putaux, M. Vignon and A. Isogai, Homogeneous suspensions of individualized microfibrils from TEMPO-catalyzed oxidation of native cellulose, *Biomacromolecules*, 2006, **7**(6), 1687–1691.

33 K. Y. Lee, T. Tammelin, K. Schulfpter, H. Kiiskinen, J. Samela and A. Bismarck, High performance cellulose nanocomposites: comparing the reinforcing ability of bacterial cellulose and nanofibrillated cellulose, *ACS Appl. Mater. Interfaces*, 2012, **4**(8), 4078–4086.

34 D. Roy, J. T. Guthrie and S. Perrier, Synthesis of natural-synthetic hybrid materials from cellulose via the RAFT process, *Soft Matter*, 2008, **4**(1), 145–155.

35 I. Siró and D. Plackett, Microfibrillated cellulose and new nanocomposite materials: a review, *Cellulose*, 2010, **17**(3), 459–494.

36 A. Nakagaito and H. Yano, Novel high-strength biocomposites based on microfibrillated cellulose having nano-order-unit web-like network structure, *Appl. Phys. A: Mater. Sci. Process*, 2005, **80**(1), 155–159.

37 A. Dufresne, D. Dupeyre and M. R. Vignon, Cellulose microfibrils from potato tuber cells: processing and characterization of starch-cellulose microfibril composites, *J. Appl. Polym. Sci.*, 2000, **76**(14), 2080–2092.

38 A. Alemdar and M. Sain, Isolation and characterization of nanofibers from agricultural residues–wheat straw and soy hulls, *Bioresour. Technol.*, 2008, **99**(6), 1664–1671.

39 A. Bhatnagar and M. Sain, Processing of cellulose nanofiber-reinforced composites, *J. Reinf. Plast. Compos.*, 2005, **24**(12), 1259–1268.

40 A. Nakagaito, S. Iwamoto and H. Yano, Bacterial cellulose: the ultimate nano-scalar cellulose morphology for the production of high-strength composites, *Appl. Phys. A: Mater. Sci. Process*, 2005, **80**(1), 93–97.

41 S. P. Lin, I. L. Calvar, J. M. Catchmark, J. R. Liu, A. Demirci and K. C. Cheng, Biosynthesis, production and applications of bacterial cellulose, *Cellulose*, 2013, **20**(5), 2191–2219.

42 S. Masaoka, T. Ohe and N. Sakota, Production of cellulose from glucose by Acetobacter xylinum, *J. Ferment. Bioeng.*, 1993, **75**(1), 18–22.

43 K. Rodríguez, P. Gatenholm and S. Renneckar, Electrospinning cellulosic nanofibers for biomedical applications: structure and in vitro biocompatibility, *Cellulose*, 2012, **19**(5), 1583–1598.

44 T. Saito, M. Hirota, N. Tamura, S. Kimura, H. Fukuzumi, L. Heux and A. Isogai, Individualization of nano-sized plant cellulose fibrils by direct surface carboxylation using TEMPO catalyst under neutral conditions, *Biomacromolecules*, 2009, **10**(7), 1992–1996.

45 J. Beecher, Organic materials: wood, trees and nanotechnology, *Nat. Nanotechnol.*, 2007, **2**, 466–467.

46 D. Dai and M. Fan, Green modification of natural fibres with nanocellulose, *RSC Adv.*, 2013, **3**, 4659–4665.

47 N. Petersen and P. Gatenholm, Bacterial cellulose-based materials and medical devices: current state and perspectives, *Appl. Microbiol. Biotechnol.*, 2011, **91**(5), 1277–1286.

48 P. R. Sharma and A. J. Varma, Functional nanoparticles obtained from cellulose: engineering the shape and size of 6-carboxycellulose, *Chem. Commun.*, 2013, **49**(78), 8818–8820.

49 K. Abe, S. Iwamoto and H. Yano, Obtaining cellulose nanofibers with a uniform width of 15 nm from wood, *Biomacromolecules*, 2007, **8**(10), 3276–3278.

50 H. P. Zhao, X. Q. Feng and H. Gao, Ultrasonic technique for extracting nanofibers from nature materials, *Appl. Phys. Lett.*, 2007, **90**(7), 073112.

51 J. Leitner, B. Hinterstoisser, M. Wastyn, J. Keckes and W. Gindl, Sugar beet cellulose nanofibril-reinforced composites, *Cellulose*, 2007, **14**(5), 419–425.

52 Q. Li, S. McGinnis, C. Sydnor, A. Wong and S. Renneckar, Nanocellulose life cycle assessment, *ACS Sustainable Chem. Eng.*, 2013, **1**(8), 919–928.





53 Q. Li and S. Renneckar, Molecularly thin nanoparticles from cellulose: isolation of sub-microfibrillar structures, *Cellulose*, 2009, **16**(6), 1025–1032.

54 M. Henriksson, G. Henriksson, L. Berglund and T. Lindström, An environmentally friendly method for enzyme-assisted preparation of microfibrillated cellulose (MFC) nanofibers, *Eur. Polym. J.*, 2007, **43**(8), 3434–3441.

55 M. Pääkkö, M. Ankerfors, H. Kosonen, A. Nykänen, S. Ahola, M. Österberg, J. Ruokolainen, J. Laine, P. Larsson and O. Ikkala, Enzymatic hydrolysis combined with mechanical shearing and high-pressure homogenization for nanoscale cellulose fibrils and strong gels, *Biomacromolecules*, 2007, **8**(6), 1934–1941.

56 M. Henriksson, L. A. Berglund, P. Isaksson, T. Lindström and T. Nishino, Cellulose nanopaper structures of high toughness, *Biomacromolecules*, 2008, **9**(6), 1579–1585.

57 T. Saito and A. Isogai, TEMPO-mediated oxidation of native cellulose: the effect of oxidation conditions on chemical and crystal structures of the water-insoluble fractions, *Biomacromolecules*, 2004, **5**(5), 1983–1989.

58 T. Saito, S. Kimura, Y. Nishiyama and A. Isogai, Cellulose nanofibers prepared by TEMPO-mediated oxidation of native cellulose, *Biomacromolecules*, 2007, **8**(8), 2485–2491.

59 S. Beck-Candanedo, M. Roman and D. G. Gray, Effect of reaction conditions on the properties and behavior of wood cellulose nanocrystal suspensions, *Biomacromolecules*, 2005, **6**(2), 1048–1054.

60 C. D. Edgar and D. G. Gray, Smooth model cellulose I surfaces from nanocrystal suspensions, *Cellulose*, 2003, **10**(4), 299–306.

61 A. Hirai, O. Inui, F. Horii and M. Tsuji, Phase separation behavior in aqueous suspensions of bacterial cellulose nanocrystals prepared by sulfuric acid treatment, *Langmuir*, 2008, **25**(1), 497–502.

62 M. M. de Souza Lima and R. Borsali, Rodlike cellulose microcrystals: structure, properties, and applications, *Macromol. Rapid Commun.*, 2004, **25**(7), 771–787.

63 C. C. Cheung, M. Giese, J. A. Kelly, W. Y. Hamad and M. J. MacLachlan, Iridescent chiral nematic cellulose nanocrystal/polymer composites assembled in organic solvents, *ACS Macro Lett.*, 2013, **2**(11), 1016–1020.

64 X. M. Dong, J. F. Revol and D. G. Gray, Effect of microcrystallite preparation conditions on the formation of colloid crystals of cellulose, *Cellulose*, 1998, **5**(1), 19–32.

65 L. Hu, G. Zheng, J. Yao, N. Liu, B. Weil, M. Eskilsson, E. Karabulut, Z. Ruan, S. Fan and J. T. Bloking, Transparent and conductive paper from nanocellulose fibers, *Energy Environ. Sci.*, 2013, **6**(2), 513–518.

66 M. Nogi, S. Iwamoto, A. N. Nakagaito and H. Yano, Optically transparent nanofiber paper, *Adv. Mater.*, 2009, **21**(16), 1595–1598.

67 G. Nyström, A. Mihranyan, A. Razaq, T. Lindström, L. Nyholm and M. Strømme, A nanocellulose polypyrrole composite based on microfibrillated cellulose from wood, *J. Phys. Chem. B*, 2010, **114**(12), 4178–4182.

68 A. Razaq, G. Nyström, M. Strømme, A. Mihranyan and L. Nyholm, High-capacity conductive nanocellulose paper sheets for electrochemically controlled extraction of DNA oligomers, *PLoS One*, 2011, **6**(12), e29243.

69 M. Iguchi, S. Yamanaka and A. Budhiono, Bacterial cellulose—a masterpiece of nature's arts, *J. Mater. Sci.*, 2000, **35**(2), 261–270.

70 H. Yano, J. Sugiyama, A. N. Nakagaito, M. Nogi, T. Matsuura, M. Hikita and K. Handa, Optically transparent composites reinforced with networks of bacterial nanofibers, *Adv. Mater.*, 2005, **17**(2), 153–155.

71 M. Nogi, K. Handa, A. N. Nakagaito and H. Yano, Optically transparent bionanofiber composites with low sensitivity to refractive index of the polymer matrix, *Appl. Phys. Lett.*, 2005, **87**(24), 243110.

72 M. J. Bonne, K. J. Edler, J. G. Buchanan, D. Wolverson, E. Psillakis, M. Helton, W. Thielemans and F. Marken, Thin-film modified electrodes with reconstituted cellulose-PDDAC films for the accumulation and detection of triclosan, *J. Phys. Chem. C*, 2008, **112**(7), 2660–2666.

73 C. N. Wu, T. Saito, S. Fujisawa, H. Fukuzumi and A. Isogai, Ultrastrong and high gas-barrier nanocellulose/clay-layered composites, *Biomacromolecules*, 2012, **13**(6), 1927–1932.

74 M. Roman and D. G. Gray, Parabolic focal conics in self-assembled solid films of cellulose nanocrystals, *Langmuir*, 2005, **21**(12), 5555–5561.

75 K. Spence, Y. Habibi and A. Dufresne, Nanocellulose-based composites, in *Cellulose Fibers: Bio- and Nano-Polymer Composites*, Springer, 2011, pp. 179–213.

76 L. Jabbour, R. Bongiovanni, D. Chaussy, C. Gerbaldi and D. Beneventi, Cellulose-based Li-ion batteries: a review, *Cellulose*, 2013, **20**(4), 1523–1545.

77 B. M. Cherian, A. L. Leao, S. F. de Souza, S. Thomas, L. A. Pothan and M. Kottaisamy, Cellulose nanocomposites for high-performance applications, in *Cellulose Fibers: Bio- and Nano-Polymer Composites*, Springer, 2011, pp. 539–587.

78 H. Dong, J. F. Snyder, D. T. Tran and J. L. Leadore, Hydrogel, aerogel and film of cellulose nanofibrils functionalized with silver nanoparticles, *Carbohydr. Polym.*, 2013, **95**(2), 760–767.

79 W. Xiao, J. Xu, X. Liu, Q. Hu and J. Huang, Antibacterial hybrid materials fabricated by nanocoating of microfibril bundles of cellulose substance with titania/chitosan/silver-nanoparticle composite films, *J. Mater. Chem. B*, 2013, **1**(28), 3477–3485.

80 I. Díez, P. Eronen, M. Österberg, M. B. Linder, O. Ikkala and R. H. Ras, Functionalization of nanofibrillated cellulose with silver nanoclusters: fluorescence and antibacterial activity, *Macromol. Biosci.*, 2011, **11**(9), 1185–1191.

81 H. S. Barud, T. Regiani, R. F. Marques, W. R. Lustri, Y. Messaddeq and S. J. Ribeiro, Antimicrobial bacterial cellulose-silver nanoparticles composite membranes, *J. Nanomater.*, 2011, **10**, 1–8.

82 G. Yang, J. Xie, F. Hong, Z. Cao and X. Yang, Antimicrobial activity of silver nanoparticle impregnated bacterial



cellulose membrane: effect of fermentation carbon sources of bacterial cellulose, *Carbohydr. Polym.*, 2012, **87**(1), 839–845.

83 G. Yang, J. Xie, Y. Deng, Y. Bian and F. Hong, Hydrothermal synthesis of bacterial cellulose/AgNPs composite: a “green” route for antibacterial application, *Carbohydr. Polym.*, 2012, **87**(4), 2482–2487.

84 L. Maria, A. L. Santos, P. C. Oliveira, A. S. Valle, H. S. Barud, Y. Messadeq and S. J. Ribeiro, Preparation and antibacterial activity of silver nanoparticles impregnated in bacterial cellulose, *Polim.: Cienc. Tecnol.*, 2010, **20**(1), 72–77.

85 W. Hu, S. Chen, X. Li, S. Shi, W. Shen, X. Zhang and H. Wang, In situ synthesis of silverchloride nanoparticles into bacterial cellulose membranes, *Mater. Sci. Eng., C*, 2009, **29**(4), 1216–1219.

86 C. Schütz, J. Sort, Z. Bacsik, V. Oliynyk, E. Pellicer, A. Fall, L. Wågberg, L. Berglund, L. Bergström and G. Salazar-Alvarez, Hard and transparent films formed by nanocellulose–TiO<sub>2</sub> nanoparticle hybrids, *PLoS One*, 2012, **7**(10), e45828.

87 C. M. Cirtiu, A. F. Dunlop-Brière and A. Moores, Cellulose nanocrystallites as an efficient support for nanoparticles of palladium: application for catalytic hydrogenation and heck coupling under mild conditions, *Green Chem.*, 2011, **13**(2), 288–291.

88 H. Koga, E. Tokunaga, M. Hidaka, Y. Umemura, T. Saito, A. Isogai and T. Kitaoka, Topochemical synthesis and catalysis of metal nanoparticles exposed on crystalline cellulose nanofibers, *Chem. Commun.*, 2010, **46**(45), 8567–8569.

89 A. Azetsu, H. Koga, A. Isogai and T. Kitaoka, Synthesis and catalytic features of hybrid metal nanoparticles supported on cellulose nanofibers, *Catalysts*, 2011, **1**(1), 83–96.

90 S. Padalkar, J. Capadona, S. J. Rowan, C. Weder, Y. H. Won, L. A. Stanciu and R. J. Moon, Natural biopolymers: novel templates for the synthesis of nanostructures, *Langmuir*, 2010, **26**(11), 8497–8502.

91 W. Wang, H. Y. Li, D. W. Zhang, J. Jiang, Y. R. Cui, S. Qiu, Y. L. Zhou and X. X. Zhang, Fabrication of bienzymatic glucose biosensor based on novel gold nanoparticles–bacteria cellulose nanofibers nanocomposite, *Electroanalysis*, 2010, **22**(21), 2543–2550.

92 P. A. Marques, H. I. Nogueira, R. J. Pinto, C. P. Neto and T. Trindade, Silver-bacterial cellulosic sponges as active SERS substrates, *J. Raman Spectrosc.*, 2008, **39**(4), 439–443.

93 R. J. Pinto, P. A. Marques, M. A. Martins, C. P. Neto and T. Trindade, Electrostatic assembly and growth of gold nanoparticles in cellulosic fibres, *J. Colloid Interface Sci.*, 2007, **312**(2), 506–512.

94 K. A. Mahmoud, K. B. Male, S. Hrapovic and J. H. Luong, Cellulose nanocrystal/gold nanoparticle composite as a matrix for enzyme immobilization, *ACS Appl. Mater. Interfaces*, 2009, **1**(7), 1383–1386.

95 L. Jabbour, C. Gerbaldi, D. Chaussy, E. Zeno, S. Bodoardo and D. Beneventi, Microfibrillated cellulose–graphite nanocomposites for highly flexible paper-like Li-ion battery electrodes, *J. Mater. Chem.*, 2010, **20**(35), 7344–7347.

96 S. Leijonmarck, A. Cornell, G. Lindbergh and L. Wågberg, Single-paper flexible Li-ion battery cells through a paper-making process based on nano-fibrillated cellulose, *J. Mater. Chem. A*, 2013, **1**(15), 4671–4677.

97 L. Zhang, X. Bai, H. Tian, L. Zhong, C. Ma, Y. Zhou, S. Chen and D. Li, Synthesis of antibacterial film CTS/PVP/TiO<sub>2</sub>/Ag for drinking water system, *Carbohydr. Polym.*, 2012, **89**(4), 1060–1066.

98 S. Ghosh, T. K. Ranebennur and H. Vasan, Study of antibacterial efficacy of hybrid chitosan-silver nanoparticles for prevention of specific biofilm and water purification, *Int. J. Carbohydr. Chem.*, 2012, **2011**, 1–11.

99 I. Díez and R. H. Ras, Few-atom silver clusters as fluorescent reporters, in *Advanced Fluorescence Reporters in Chemistry and Biology II*, Springer, 2010, pp. 307–332.

100 Y. H. Ngo, D. Li, G. P. Simon and G. Garnier, Effect of cationic polyacrylamides on the aggregation and SERS performance of gold nanoparticles-treated paper, *J. Colloid Interface Sci.*, 2013, **392**, 237–246.

101 Y. Wang, H. Wei, B. Li, W. Ren, S. Guo, S. Dong and E. Wang, SERS opens a new way in aptasensor for protein recognition with high sensitivity and selectivity, *Chem. Commun.*, 2007(48), 5220–5222.

102 X. M. Qian and S. Nie, Single-molecule and single-nanoparticle SERS: from fundamental mechanisms to biomedical applications, *Chem. Soc. Rev.*, 2008, **37**(5), 912–920.

103 W. Leng and P. J. Vikesland, Nanoclustered gold honeycombs for surface-enhanced Raman scattering, *Anal. Chem.*, 2013, **85**(3), 1342–1349.

104 A. Chiappone, J. R. Nair, C. Gerbaldi, L. Jabbour, R. Bongiovanni, E. Zeno, D. Beneventi and N. Penazzi, Microfibrillated cellulose as reinforcement for Li-ion battery polymer electrolytes with excellent mechanical stability, *J. Power Sources*, 2011, **196**(23), 10280–10288.

105 F. Alloin, A. D'Aprea, N. E. Kissi, A. Dufresne and F. Bossard, Nanocomposite polymer electrolyte based on whisker or microfibrils polyoxyethylene nanocomposites, *Electrochim. Acta*, 2010, **55**(18), 5186–5194.

106 M. Schroers, A. Kokil and C. Weder, Solid polymer electrolytes based on nanocomposites of ethylene oxide-epichlorohydrin copolymers and cellulose whiskers, *J. Appl. Polym. Sci.*, 2004, **93**(6), 2883–2888.